Tr. J. of Physics
22 (1998) , 69 – 76.

Microscopic Calculations of the Nucleus-Nucleus Optical Potential

M. M. OSMAN
Physics Department, Faculty of Science,
Cairo University
Giza, EQYPT

Received 19.11.1996

Abstract

In present work, a density dependent nucleon-nucleon interactions based on the G-matrix elements of the Paris nucleon-nucleon potential have been used to calculate the real part of the nucleus-nucleus optical potential. We have compared our results with those deduced from experiment. We found that our results, obtained using a suitable approximation of the kinetic energy density, agree satisfactory with those extracted from experiment at the strong absorption radius. Moreover, the higher values of the compressibility, K, agree better with experiment than the lower values.

Introduction

Recently Khoa and von Oertzen [1] proposed three density and energy dependent nucleon-nucleon (NN) forces that correspond to three different values of the compressibility of nuclear matter. These forces reproduced correctly both the features of the normal nuclear matter and the microscopic results for the nucleon optical-model potential. They were used to fit the recent heavy ion (HI) scattering data and to determine the nuclear equation of state of cold nuclear matter. The latter is important in both nuclear physics and astrophysics [2]. More application of these forces to other nuclear phenomena is needed.

The aim of the present work is to examine to what consistently appears in nuclear matter study as the microscopic derivation of the heavy ion optical potential. For this purpose we used the so called M3Y NN interaction based on the G-matrix element of the Paris [3] (M3Y-paris) potential and its density and energy dependent versions, derived in Ref. [1], to calculate the real part of the nucleus-nucleus interaction potential at strong absorption radius (R_s), for different pairs of interacting nuclei.

In section 2 we briefly present the derivation of the real HI optical potential using an approximation based on the DME method. Our results are given in section 3.

Formalism

The energy dependent real part of the HI potential at a separation distance R between the centers of the two ions is obtained by

$$U(E,R) = U_D(E,R) + U_{EX}(E,R), \tag{1}$$

where $U_D(E,R)$ and $U_{EX}(E,R)$ are the energy-dependent direct and exchange parts of the HI potential. $U_D(E,R)$ is obtained by using the usual folding method [4]:

$$U_D(E,R) = \int \rho_1(\vec{r}_1)\rho_2(\vec{r}_2)V_D(\rho,E,s)d\vec{r}_1\, d\vec{r}_2, \quad \vec{s} = \vec{r}_2 - \vec{r}_1 + \vec{R}. \tag{2}$$

$U_{EX}(E,R)$ is calculated within a generalized version of the double folding model [5],

$$U_{EX}(E,R) = \int \rho_1(\vec{r}_1, \vec{r}_1 + \vec{s})\rho_2(\vec{r}_2, \vec{r}_2 + \vec{s})V_{EX}(\rho,E,s)\exp\left(\frac{i\vec{K}(R)\cdot\vec{s}}{M}\right) d\vec{r}_1\, d\vec{r}_2. \tag{3}$$

In equations (2) and (3) $V_D(\rho,E,s)$ and $V_{EX}(\rho,E,s)$ are the density and energy dependent direct and exchange parts of the effective NN force, ρ_1 and ρ_2 are the densities of the two colliding nuclei and $K(R)$ is the relative-motion momentum given by [5],

$$K^2(R) = \frac{2mM}{\hbar^2}[E_{C.M} - U(E,R) - V_C(R)]. \tag{4}$$

Here, $M[= A_P A_T/(A_P + A_T)]$ and $E_{C.M}$ are the reduced mass and the relative energy in the center of mass system, respectively. m and $V_C(R)$ are the nucleon mass and the coulomb potential. In order to simplify the numerical calculation of $U_{EX}(E,R)$, many authors [1, 2, 5, 6] have used an approximation [7] for the density matrix derived from the DME method of Negate and Vautherin [8]. This approximation is

$$\rho(\vec{R}, \vec{R} + \vec{s}) = \rho\left(\vec{R} + \frac{1}{2}\vec{s}\right)\hat{j}_1\left(K_{eff}\left(\vec{R} + \frac{1}{2}\vec{s}\right)s\right) \tag{5}$$

with $\hat{j}_1(x) = 3(\sin x - x\cos x)/x^3$ and,

$$K_{eff}^2 = \frac{5}{3\rho(r)}\left[\tau(r) - \frac{1}{4}\nabla^2\rho(r)\right]. \tag{6}$$

Usually, $\tau(r)$ is calculated using one of the two approximations

$$\tau(r) = \frac{3}{5}K_f^2\rho(r) + \frac{1}{3}\nabla^2\rho(r) + \frac{1}{36}\frac{|\vec{\nabla}\rho(r)|^2}{\rho(r)} \tag{7a}$$

$$\tau(r)=\frac{3}{5}K_f^2\rho(r)+\frac{1}{3}\nabla^2\rho(r)+\frac{1}{4}\frac{|\vec{\nabla}\rho(r)|^2}{\rho(r)}. \tag{7b}$$

The first term in each approximation is the Thomass-Fermi term with

$$K_f^2=\left[\frac{3}{2}\pi^2\rho(r)\right]^{2/3}.$$

The two equations (7a) and (7b) are derived from the extended Thomas-Fermi approximation which is given by

$$\tau(r)=\frac{3}{5}K_f^2\rho(r)+\frac{1}{3}\nabla^2\rho(r)+C_s\frac{|\vec{\nabla}\rho(r)|^2}{\rho(r)}.$$

The third term is the so-called Weizsacker term with strength C_s. It represents the contribution of $\tau(r)$ from the surface of the nucleus. Normally one takes $C_s=\frac{1}{36}$ for a finite fermionic system (Equation (7a)). Many authors [6] have used this value together with the ordinary M3Y force to derive the real optical potential. A detailed study by Baltin [9] has shown that, in a region of small density, the value of C_s should be $C_s=\frac{1}{4}$ (Equation (7b)). This value has been used to derive the ion-ion potentials in refs. [2, 5].

Our choice for the NN interaction $V_{D(EX)}(\rho,E,s)$ is the so-called density and energy dependent NN interaction. It is given by [1-2],

$$V_{D(EX)}(\rho,E,s)=f(\rho)g(E)V_{D(EX)}(s), \tag{8}$$

where $V_{D(EX)}(s)$ is the so-called M3Y-paris interaction [2] given by,

$$V_D(s)=11061.625\frac{\exp(-4s)}{4s}-2537.5\frac{\exp(-2.5s)}{2.5s} \tag{9a}$$

$$V_{EX}(s)=-1524.25\frac{\exp(-4s)}{4s}-518.75\frac{\exp(-2.5s)}{2.5s}-7.8474\frac{\exp(-0.7072s)}{0.7072s} \tag{9b}$$

and

$$f(\rho)=C(1-\alpha\rho^{\beta}). \tag{10}$$

Here, $\rho=\rho_1+\rho_2$ and the parameters C,α and β are taken from ref. [2]. $g(E)$ in equation (8) is given by,

$$g(E)=(1-0.003E). \tag{11}$$

E is the energy per projectile nucleon in laboratory system [11].

Results and Discussion

The total ion-ion potential $U(R)$ is obtained from equation (1) by using the iteration procedure [2]. In our calculations, we used the so-called M3Y-paris NN force and its density and energy dependent forces denoted by BDM3Y1, BDM3Y2 and BDM3Y3 derived in Ref. [1]. The density dependent NN forces BDM3Y1, BDM3Y2 and BDM3Y3 correspond to the values of nuclear matter compressibility 210.6,332.1 and 453.6 MeV, respectively. The matter distribution of either the two colliding nuclei was approximated by the Fermi shape,

$$\rho(r) = \frac{\rho_0}{1 + \exp[(r - R_0)/a]},$$

where the parameters ρ_0, R_0 and a are taken from Ref. [4]. Let us denote the HI potential $U(R)$ calculated using equation (1) with $\tau(r)$ defined by equations (7a) and (7b) by $U_1(R)$ and $U_2(R)$, respectively.

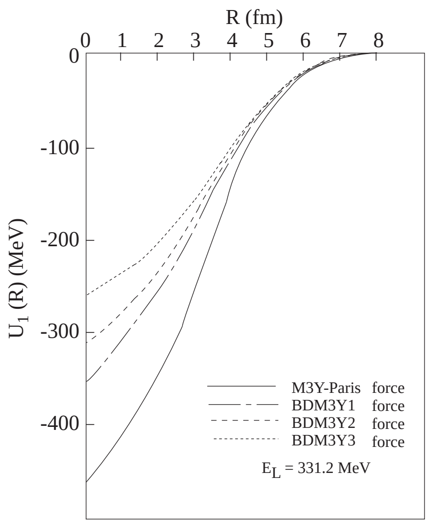

Figure 1. The real part of the optical potential $U_1(R)$ for the nuclear pair $O^{16} - O^{16}$ calculated at $E_L = 331.2$ MeV using three density dependent interactions and the conventional M3Y-paris force.

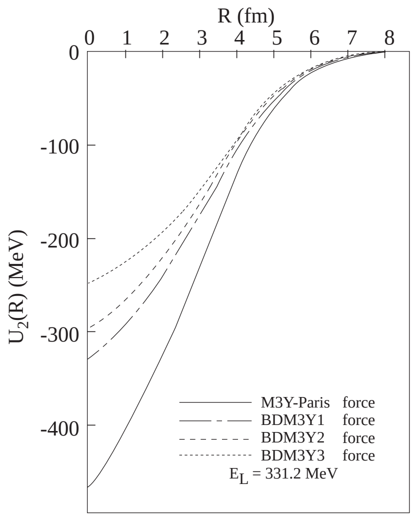

Figure 2. The same as Figure 1 for the potential $U_2(R)$.

Figures (1) and (2) show the potentials $U_1(R)$ and $U_2(R)$ for the nuclear pair $O^{16} - O^{16}$ at energies $E_L = 82.88, 331.2$ and 745.6 MeV for three values of the HI separation distance. The figures and the table show that both $U_1(R)$ and $U_2(R)$ become more repulsive as the value of the nuclear compressibility increases. Also, the three density dependent NN forces produce more repulsive potentials compared with that derived from M3Y-paris force. For all NN forces the potential $U_1(R)$ calculated with approximation (7a) for $\tau(r)$ is slightly attractive than the other HI potential $U_2(R)$. In ref. [1] calculated cross sections and the experimental data for $O^{16} - O^{16}$ system are ploted versus qR using a different type of the optical potential, where q is the linear momentum transfer and $R = 2/times 16^{1/3} 16^{1/3} fm$. From this plote one can clearly see that the BDM3Y1 potentials are the best choice of the real folded potentials. As we have mentioned before, the aim of the present calculations is to show that the NN force can be used for a consistent description of the nuclear matter properties and the derivation of HI optical potential. For this purpose we have calculated the HI potential at the strong absorption radius R_s for 10 ion-ion scattering cases in the energy range 3-20 MeV/nucleon. Also, we consider 3 cases with Ar^{40} as a projectile at energy 44 MeV/nucleon.

Our result are given on Table 2 for the optical potential $U_1(R_s)$ and on Table 3 for the potential $U_2(R_s)$. Table 2 shows that the data can be summarized in the energy range 3-20 MeV/nucleon by the normalization factor $N = 0.88 \pm 0.11$ for the force M3Y-paris, $N_1 = 0.80 \pm 0.10$ for the force BDM3Y1, $N_2 = 0.86 \pm 0.11$ for the force BDM3Y2 and $N_3 = 0.89 \pm 0.12$ for the force BDM3Y3. For Ar^{40} data at energy 44 MeV/nucleon the normalization factors required are $N = 0.65 \pm 0.05$, $N_1 = 0.58 \pm 0.05$, $N_2 = 0.62 \pm 0.05$ and $N_3 = 0.66 \pm 0.05$. Table 3 also shows that the potential $U_2(R_s)$ can be normalized on the energy range 3-20 MeV/nucleon by the factors $N = 0.97 \pm 0.12$ for the M3Y-paris force, $N_1 = 0.88 \pm 0.11$ for the force BDM3Y1, $N_2 = 0.94 \pm 0.12$ for the force BDM3Y2 and $N_3 = 0.99 \pm 0.12$ for the force BDM3Y3. For Ar^{40} data at energy 44 MeV/nucleon, these normalization factors are $N = 0.69 \pm 0.05, N_1 = 0.63 \pm 0.04, N_2 = 0.68 \pm 0.04, N_3 = 0.70 \pm 0.05$. The Tables 2 and 3 show that the ion-ion potential $U_2(R)$ is better than $U_1(R)$ in predicting the experimental data at the strong absorption radius. The tables show also that the higher values of the compressibility, K, agree better with experiment than the lower values. Thus the effect of compressibility on both $U_1(R_s)$ and $U_2(R_s)$ is opposite to the density effect on M3Y interaction.

Table 1. A comparison between the ion-ion potentials $U_1(R)$ and $U_2(R)$ calculated in the relvent tail region for the nuclear pair $O^{16} - O^{16}$. The table shows this comparison at three different energies in the laboratory system by using the so-called M3Y-paris nucleon-nucleon force and its density and energy dependent interactions BDM3Y1, BDM3Y2, BDM3Y3.

		M3Y		BDM3Y1		BDM3Y2		BDM3Y3	
E_{lab} MeV	R fm	U1	U2	U1	U2	U1	U2	U1	U2
	4	-153.55	-143.27	-129.53	-124.81	-119.57	-115.06	-113.37	-109.5
82.88	6	-23.34	-20.8	-22.89	-22.09	-20.17	-19.52	-19.6	-19.1
	8	-1.34	-1.23	-1.47	-1.34	-1.31	-1.22	-1.3	-1.22
	4	-141.57	-133.36	-111.33	-104.00	-107.23	-99.91	-102.2	-94.94
331.2	6	-21.78	-133.36	-19.91	-17.97	-19.25	-17.41	-18.82	-17.03
	8	-1.24	-1.18	-1.32	-1.21	-1.23	-1.15	-1.20	-1.14
	4	-124.64	-118.8	-103.8	-99.61	-98.3	-94.21	-94.5	-89.15
745.4	6	-19.74	-18.47	-19.08	-18.47	-17.72	-17.18	-17.07	-16.85
	8	-1.21	-1.15	-1.27	-1.17	-1.16	-1.07	-1.12	-1.04

Table 2. The normalization factors required for $U_1(R_s)$ to fit the experimental data at the strong absorption radius R_s. N, N_1, N_2 and N_3 are the normalization factors for the forces M3Y-paris, BDM3Y1, BDM3Y2 and BDM3Y3 respectively.

PAIR	E_L MeV	R fm	N	N_1	N_2	N_3
$C^{12} - Ca^{40}$	45.0	9.00	0.81	0.75	0.80	0.83
$C^{12} - Ca^{40}$	51.0	9.10	0.75	0.68	0.74	0.77
$C^{12} - Zr^{90}$	98.0	10.0	0.80	0.73	0.76	0.79
$C^{12} - pb^{208}$	96.0	12.2	9.00	0.99	1.06	1.13
$O^{16} - Ca^{40}$	74.4	9.3	9.10	0.75	0.82	0.85
$O^{16} - Ni^{60}$	61.4	10.1	10.0	0.91	0.99	1.03
$O^{16} - Ni^{60}$	141.7	9.60	0.98	0.89	0.96	1.00
$O^{16} - pb^{208}$	192.0	12.4	0.82	0.76	0.79	0.80
$O^{16} - pb^{208}$	312.6	12.1	0.95	0.87	0.90	0.93
$Ca^{40} - Ca^{40}$	143.6	10.7	0.77	0.69	0.74	0.76
$Ar^{40} - Ni^{60}$	1760.	10.15	0.58	0.54	0.57	0.59
$Ar^{40} - Sn^{120}$	1760	11.55	0.66	0.59	0.62	0.67
$Ar^{40} - pb^{208}$	1760	12.9	0.70	0.61	0.68	0.71

Table 3. The same as Table 2 but for $U_2(R_s)$

PAIR	E_L MeV	R fm	N	N_1	N_2	N_3
$C^{12}-Ca^{40}$	45.0	9.00	0.91	0.83	0.89	0.92
$C^{12}-Ca^{40}$	51.0	9.10	0.83	0.75	0.81	0.85
$C^{12}-Zr^{90}$	98.0	10.0	0.88	0.80	0.87	0.90
$C^{12}-pb^{208}$	96.0	12.2	1.22	1.10	1.17	1.26
$O^{16}-Ca^{40}$	74.4	9.3	0.92	0.83	0.90	0.93
$O^{16}-Ni^{60}$	61.4	10.1	1.11	1.00	1.08	1.13
$O^{16}-Ni^{60}$	141.7	9.60	1.07	0.98	1.05	1.09
$O^{16}-pb^{208}$	192.0	12.4	0.90	0.83	0.86	0.90
$O^{16}-pb^{208}$	312.6	12.1	1.03	0.93	0.97	1.01
$Ca^{40}-Ca^{40}$	143.6	10.7	0.86	0.75	0.81	0.86
$Ar^{40}-Ni^{60}$	1760.	10.15	0.63	0.58	0.62	0.63
$Ar^{40}-Sn^{120}$	1760	11.55	0.70	0.65	0.69	0.71
$Ar^{40}-pb^{208}$	1760	12.9	0.74	0.67	0.72	0.75

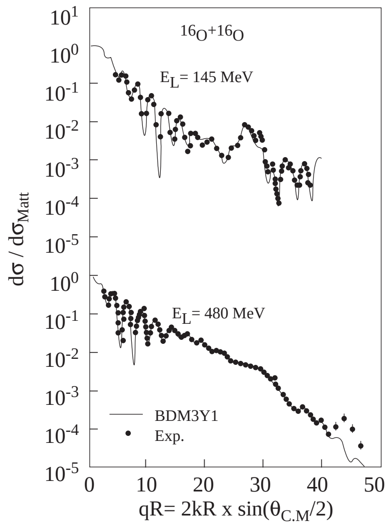

Figure 3. Fits to the elastic $O^{16}-O^{16}$ scattering data at $E_L=145$ and 480 MeV using the density dependent interaction BDM3Y1 (see Ref. [1]).

Comparing the normalization factor for the ordinary M3Y-paris NN force with the corresponding normalization of the BDM3Y family, one can say that the BDM3Y forces which are derived by fitting both the nuclear matter and the nucleon-nucleus optical potential data is also successful when applied to HI scattering. This shows that it is possible to derive a nucleon-nucleon forces for consistent description of both nuclear matter and scattering data.

References

[1] Khoa, Dao T. and von Oertzen, W., Phys. Lett., **B304** (1993) 8.

[2] Khoa, Dao T., et.al., Phys. Rev. Lett., **74** (1995) 34.
Khoa, Dao T., and Von Oertzen, W., Phys. Lett., **B342** (1995) 6.

[3] Anantarman, N., Tok, H. and Bertsch, G.F., Nucl. Phys., **A398** (1983) 269.

[4] Satcher, G.R. and Love, W.G. Phys. Rep. **55** (1979) 183.

[5] Khoa, Dao T., W. von Oertzen and Bohlen, H.G., Phys. Rev., **C49** (1994) 1652.

[6] Chaudhuri, A.K. and Sihna, B., Nucl. Phys. **A455** (1986) 169.
Chaudhuri, A.K., Basu,D.N. and Sinha, B., Nucl. Phys., **A439** (1985) 415.

[7] Campi, X. and Bouysoy, A., Phys. Lett., **B73** (1978) 263.

[8] Negele, J.W. and Vautherin, D., Phys. Rev., **C5**, (1972) 1472; **C11** (1975) 1031.

[9] Baltin, R., Naturforsch, Z., **27 A** (1972) 1176.